Nuclear Materials and Energy 9 (2016) 480–483

Contents lists available at ScienceDirect

Nuclear Materials and Energy

journal homepage: www.elsevier.com/locate/nme

Effect of neutron irradiation on the microstructure of tungsten

M. Klimenkov[a,*], U. Jäntsch[a], M. Rieth[a], H.C. Schneider[a], D.E.J. Armstrong[b], J. Gibson[b], S.G. Roberts[b]

[a] Karlsruhe Institute of Technology (KIT), Institute for Applied Materials, 76021 Karlsruhe, Germany
[b] University of Oxford, Department of Materials, Oxford, UK

ARTICLE INFO

Article history:
Available online 14 October 2016

Keywords:
Tungsten
Neutron irradiation
Microstructure
Transmutation

ABSTRACT

Two grades of pure tungsten, single and polycrystalline, were irradiated for 282 days in the HFR reactor, Petten, at 900 °C to an average damage level of 1.6 dpa. Each grade of tungsten was investigated using the transmission electron microscope (TEM) to assess the effect of neutron irradiation on tungsten microstructure. Investigations revealed the formation of faceted cavities, whose diameter varies from 4 to 14 nm in both materials. The cavities are homogeneously distributed only inside single crystalline tungsten. The local distribution of cavities in polycrystalline tungsten is strongly influenced by grain boundaries. The number densities of cavities were measured to be 4×10^{21} m^{-3} for polycrystalline and 2.5×10^{21} m^{-3} for single crystalline tungsten. This corresponds to volumetric densities of 0.45% and 0.33% respectively. High-resolution transmission electron microscopy (HRTEM) revealed that faces of cavities are oriented in (110) plane. Analytical investigations showed precipitation of rhenium and osmium produced by a transmutation reaction around cavities and at grain boundaries.

1. Introduction

Tungsten (W) is considered to be the most promising choice for the plasma-facing component of fusion reactors because of its favourable properties, such as a high melting point, high sputtering resistivity, and high temperature strength. Due to the high melting temperature of W, even for the very high expected operating temperature for W in fusion reactors significant irradiation-induced damage is expected [1,2].

Characterisation of microstructural and mechanical properties of neutron-irradiated W was covered by several publications in the past [3–5]. In most studies W was irradiated with doses of less than 1.5 dpa in the 400–800 °C temperature range. An extensive microstructural study and review of irradiated pure W and W-*Re* alloys was performed by Hasegawa et al. [4]. The results published in numerous papers are summarised in the diagram which shows defect formation depending on radiation dose and temperature [4]. Analysing this Hasegawa-diagram can be concluded that irradiation of pure W at 800 °C to doses higher as 1 dpa leads to the formation of cavities only. Microstructures with both dislocation loops and cavities were observed only at irradiation doses down to 0.5 dpa. Current results relating to the W microstructure after 1.6 dpa irradiation at 900 °C are beyond the temperature and radiation ranges of Hasegawa-diagram [4] and, hence, can be considered a complement to the already published results.

Irradiation in the sub-dpa ranges does not lead to a significant accumulation of rhenium (*Re*) or osmium (Os). In former studies W-*Re* or W-*Re*-Os alloys were neutron-irradiated in order to simulate the influence of transmutation-induced elements on the microstructure and mechanical properties [3,5,6]. As was shown, the presence of *Re* influences the formation of cavities and contributes to the increased hardening of material.

Single crystalline and polycrystalline W specimens were subjected to neutron irradiation in the High Flux Test Reactor (HFR) up to a dose of 1.6 dpa at 900 °C in order to evaluate microstructural changes, including formation of radiation-induced cavities as well as precipitation of *Re* and Os produced by a complex chain of transmutation reactions. Imaging of the two-dimensional distribution of these elements allows conclusions to be drawn with respect to their influence on the microstructure under real working conditions.

2. Experimental

The single crystalline and polycrystalline samples of commercially pure W from Metals Crystal and Oxides Limited, Cambridge,

* Corresponding author. Fax: +49 721 608 24567.
E-mail address: michael.klimenkov@kit.edu (M. Klimenkov).

http://dx.doi.org/10.1016/j.nme.2016.09.010

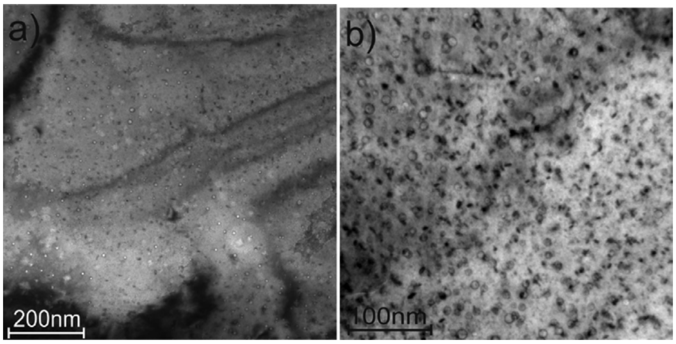

Fig. 1. TEM images of single crystal material obtained with different magnifications.

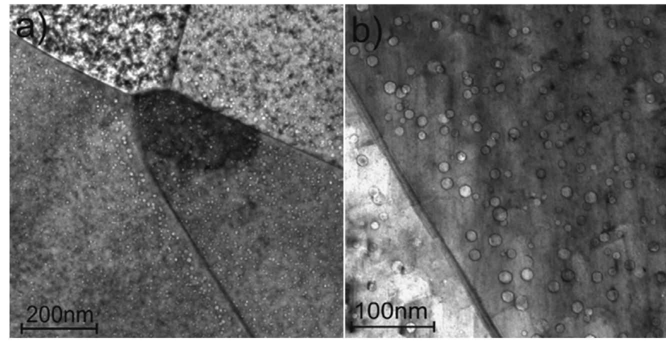

Fig. 2. TEM images of polycrystalline material obtained with different magnifications.

UK were irradiated for 208 days positioned in two different locations in the High Flux Reactor (HFR), Petten, at 900 °C. The materials were also used in previous studies published in refs. [7–9]. The total neutron flux was 6.8×10^{18} m^{-2}s^{-1} (3.2×10^{18} m^{-2}s^{-1}, E < 0.1 MeV) for the first location (148 full power days) and 6.6×10^{18} m^{-2}s^{-1} (3.2×10^{18} m^{-2}s^{-1}, E < 0.1 MeV) for the second location (60 full power days). The samples were positioned next to another experiment with very strong neutron absorption properties, so that material was exposed to a lower than normal for HFR fraction of thermal neutrons. Inventory simulation was performed with FISPACT-II [10] of pure W taking into consideration detailed irradiation schedule and neutron spectrum.

The *Re* and Os concentrations in irradiated W were calculated to 1.4% and 0.1% respectively. The calculated *Re* concentration (C_{Re}) is in the good agreement with 1.2–1.4 wt.% values from quantitative energy dispersive x-ray (EDX) measurements in TEM performed by comparison of W-L_α (8.40 keV) and *Re*-L_α (8.65 keV) line intensities (I) using $C_{Re}=C_W\times(I_{Re}/I_W)$ equation. The estimated statistical error of 20% for the measurement of *Re*-L_α line intensity makes the consideration of Cliff-Lorimer $k_{WRe}=0.987$ factor for quantification not useful. The radiation damage was calculated to 1.6 dpa in the W using displacement threshold of $E_d = 55$ eV

Post-irradiation microstructural examination of both materials was performed in the Fusion Materials Laboratory (FML) at KIT. Thin foils for TEM investigations were prepared using the FIB technique and deposited on a molybdenum grid. The flash polishing (12V×50 ms) was applied to remove surface radiation damage after FIB preparation. TEM characterisation was performed using an FEI Tecnai 20 FEG microscope with an accelerating voltage of 200 kV, a scanning unit for performing scanning TEM (STEM) with a high-angle annular dark field (HAADF) detector, and an EDAX energy dispersive x-ray (EDX) detector for elemental analysis. The analytical investigations by STEM-EDX were made with a beam size of 1.0–1.5 nm.

3. Results

The TEM images show the formation of nano-sized faceted cavities in both poly-crystalline and single crystal materials (Figs. 1, 2). The images were obtained from the grains with crystallographic orientation fare from low indexed zone axes near to two-beam conditions. Such orientation in the bright field mode makes possible contrast-rich imaging of structural defects. The cavities and needle shaped *Re*-rich precipitates with typical size 3nm×15 nm are homogeneously distributed in the single crystal material (Fig. 1a,b). The *Re*-rich precipitates have approximately the same number density as cavities. The spatial distribution of cavities in polycrystalline material is influenced by grain boundaries. A 20 nm thick zone denuded of cavities was observed adjacent to both sides of grain boundaries. No cavity has been detected direct at the grain boundaries (Fig. 2a, b). The histograms which reveal the size distribution of cavities in both materials are shown in Fig. 3. Their diameter varies from 3 to 14 nm with an average value 5–5.5 nm. The fraction of cavities with diameter larger than 10 nm is higher in the polycrystalline than in single crystal material. The largest cavities have been formed in the area near to the grain boundary. The number densities of cavities are measured to be 4×10^{21} m^{-3} for the polycrystalline material and 2.5×10^{21} m^{-3} for the single crystalline material. This corresponds to volumetric densities of 0.45% for the polycrystalline material and 0.38% for the single crystal material, respectively. The cavities with sizes larger than 10 nm have been formed in the area near to the grain boundaries in polycrystalline material. The thickness of TEM foils was measured to 45 nm in Fig. 1a and 110 nm in Fig. 2a. This difference in the thicknesses is the reason for visible much higher number density of cavities in polycrystalline material by comparison Figs. 1a and 2a.

The cavities often show a faceted structure which reflects their orientation in the matrix. Fig. 4 shows the high-resolution TEM (HRTEM) micrograph of a 6 nm cavity in a grain oriented with [110] zone axis (a) together with the corresponding fast Fourier transformation (FFT) image (b). The imaged atomic planes of (110) and (200) types with $d_{110} = 2.26$ nm and $d_{200} = 1.62$ nm correspond to the cubic structure of W. These results show that the void's facets are preferably formed in the 110 plane. The faceted shape is well visible in cavities which diameter is larger than 5 nm, whereas cavities with diameter smaller than 5 nm rather exhibit a round shape in TEM images.

In addition to the formation of structural defects or cavities, the production of transmutation elements, such as *Re* and Os, was observed after neutron irradiation of W [3]. The EDX mesurements obtained from the area of several microns show that originally pure W contains 1.3% *Re* and > 0.5% Os after irradiation in HFR. This value is in the good agreement with caculations Irradiation-induced precipitation of these elements may influence the mechanical properties and microstructure of W, as previosuly observed in ion iarradiated W-*Re* and W-*Re*-Os alloys [11,12]. To identify the *Re* distribution, two-dimensional EDX analysis with a fine electron probe, whose diameter was approximately 1 nm, was performed (Figs. 5, 6). The cavities are visible in HAADF images as dark spots (Figs. 5a, 6a). The scanned area in the polycrystalline material, which is marked by a square, includes a triple point at the grain boundaries (Fig. 5). The W and *Re* maps demonstrate that *Re* is preferably located at structural defects, such as grain boundaries and around cavities. The quantitative analysis of EDX spectra shows that *Re* concentration at the grain boundary can be estimated to be in the 12%−18% range. In some cavities a *Re*-rich circle can be recognised. This circle has been formed around each, even the smallest, void. The density of *Re*-rich precipitates in the single crystal material is approximately 2 times higher than that of